A SYSTEM FOR AUTOMATIC AERIAL TRIANGULATION

Rüdiger Brand, Christian Heipke
Chair for Photogrammetry and Remote Sensing
Technische Universität München, D–80290 Munich, Germany
Tel: +49-89-2892-2673, Fax: +49-89-2809573
E-mail: {ruediger}{chris}@photo.verm.tu-muenchen.de

Commission II, Working Group 8

KEY WORDS: AAT, image matching, manifold conjugate points, block adjustment,

ABSTRACT

During the last years a system for automatic aerotriangulation (AAT) was developed at the Technische Universität München. This paper describes the current state of our approach.
Our approach is characterized by highly redundant hierarchical feature based matching using points at arbitrary positions within the images, a tight coupling of matching and robust block adjustment and focusses on obtaining a large number of manifold conjugate points which are determined during the matching process. A new concept for the determination of manifold conjugate point tuples was introduced recently, namely a RANSAC (Random Sample Consensus) algorithm followed by checks for geometric consistency.
The approach has been tested with three data sets of the OEEPE-ISPRS test "Performance of tie point extraction in automatic aerial triangulation" and two further examples. The results of a subsequent robust bundle block adjustment lie between 0.3 and 0.4 pixel for the standard deviation of all image coordinates, which is reasonable since only feature based matching is performed. The calculated exterior orientation parameters are proved during the OEEPE-ISPRS test evaluation. Furthermore the geometric block stability is very good due to the large amount of tie points and in particular due to the large amount of multi-ray points.

1 INTRODUCTION

In the last years there has been considerable research and developement in automatic aerial triangulation (AAT, see e.g. Lue 1996; Miller et al. 1996; Ackermann, Krzystek 1997; Schenk 1997; Tang et al. 1997). One of the developements is carried out at Technische Universität München. Its system is an extension of a system for automatic relative orientation of aerial imagery (Tang, Heipke 1996) which has been implemented into a commercial digital photogrammetric system and is used in daily practice. This paper describes the current state of our research.

A new concept for the generation of the manifold conjugate point tuples based on graph theory and probability theory was recently developed and is discussed in detail in this paper. The general concept of our system is presented in (Heipke et al 1997) and is only reviewed briefly here (see Figure 1). It can handle both central perspective and 3-line geometry, althought only frame imagery is discussed in the remaining part of this paper. Our AAT-approach uses point features and a coarse-to-fine strategy based on image pyramids. After extracting a large amount of point features in each image using the Förstner interest operator a feature based matching algorithm is applied to all image pairs. Then the manifold conjugate point tuples are generated and checked for geometric consistency. Subsequently, the exterior orientation parameters for the whole block are calculated in a highly redundant robust bundle adjustment together with 3D-coordinates for the conjugate point tuples. This information serves as initial values on the next lower pyramid level. Our approach is divided into two different phases. During the first phase from the start level to the intermediate pyramid level the processing is carried out on the whole images. During the second phase from the intermediate level to the final level instead of the whole images only image chips around tie points extracted earlier are processed. In order to generate a maximum of multi-ray points the corresponding tracking of the points from one pyramid level to the next lower one is performed by backprojecting each model point into all available images of the lower level, not only in those where the tie point was extracted in the higher level.

The new concept for the generation of point tuples is outlined in Section 2. Experimental results for three data sets of the OEEPE-ISPRS test "Performance of tie point extraction in automatic aerial triangulation" (Heipke, Eder 1996) and two other examples are presented in Section 3. Conclusions and further developements to our approach are discussed in the last section.

2 NEW CONCEPT

In this section we give a detailed description of the new concept for the generation of manifold conjugate point tuples.

After matching all overlapping images pairwise in all combinations an undirected graph is generated. The nodes of the graph are the point features, the edges are the matches between them. Similar to (Tsingas 1992) this graph is divided into connected components. A standard method for this task is the depth first search (DFS, Turau 1996). All further operations are applied to each resulting subgraph separately.

The next step is the generation of the point tuples. One point tuple is characterized by the property that not more than one feature per image is admissible. This problem can be solved by complete search or tree search algorithms or

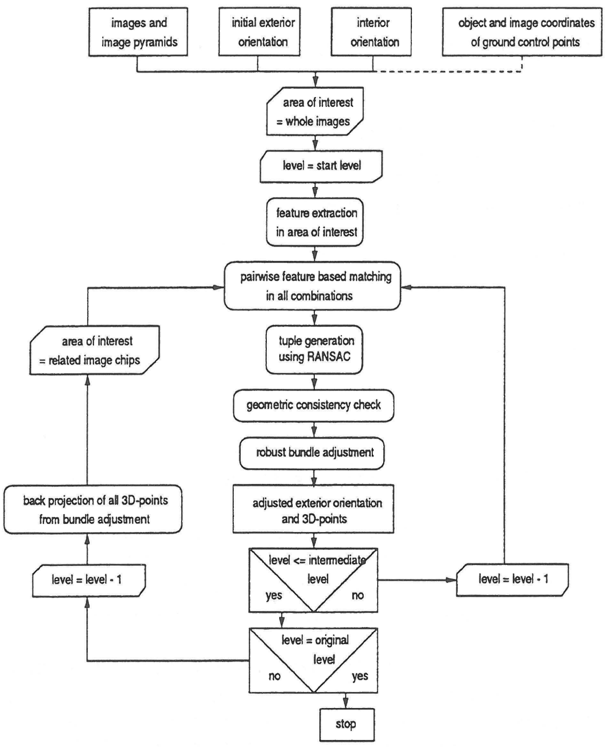

Figure 1: Flow chart of the AAT-approach

binary programming techniques (Tsingas 1992). Most of these algorithms do not use geometric constraints. They also divide the tasks of generation of multiple matches and the detection of mismatches into separate subtasks. We pursue another strategy and include a geometric consistency check in our algorithm for the generation of multiple matches. The challenge of generating multiple points lies in the fact that each subgraph usually contains a large amount of blunders.

RANSAC (Random Sample Consensus, Fischler, Bolles 1981) is a method, which has been shown to successfully deal with this challenge (see e.g. Schickler 1992). The method relies on the fact that the likelihood of hitting a good configuration (tuple) by randomly choosing a set of observations (features of the subgraph) is large after a certain number of trials. In our approach the RANSAC procedure can be described as follows :

1. Choose one edge of the subgraph (one matching pair) randomly.
2. Calculate the model coordinates of the point by forward intersection using initial values of the exterior orientation parameters.
3. Transform the model point into all images.
4. Calculate the residuals in image space of all nodes (features) in the subgraph and the standard deviation σ_0 of the node coordinates from the residuals.
5. Choose for each image the feature with the smallest residuals provided both, the values in x and y, are smaller than $3\sigma_0$.
6. Repeat step 2 and 3 with all remaining observations.
7. Calculate the residuals in image space of all observations and the standard deviation σ_0 of the node coordinates from the residuals.
8. Check the tuple according to the accuracy of the level, which is defined as $\sigma_0 = 6 * pixelsize$ for the start level and $\sigma_0 = 2/3 * pixelsize$ for all other levels.

Steps 1–8 are repeated for a given number of trials, which is calculated depending on the size of the subgraphs. A further improvement, not implemented yet, is expected from iteratively carrying out steps 6 and 7 while weighting observations with large residuals. At the end of the algorithm the best tuple is selected according to the number of images, in which the point was found, and the mean interest value of the features. Subsequently the next subgraph is processed. The RANSAC procedure is utilised for each subgraph on each pyramid level.

3 EXPERIMENTAL RESULTS

The experimental test is performed with three data sets of the OEEPE-ISPRS test "Performance of tie point extraction in automatic aerial triangulation" and two other examples. A detailed description of the test data sets can be found in (Heipke et al. 1998), the other two examples are Manhattan and Forssa (Heipke et al. 1997). A short description of the test data is given in Table 1.

For the test imagery information on the camera calibration, the pixel coordinates of the fiducial marks, initial values for the exterior orientation parameters accurate to about 50 m for the projection center and 2° for the angles, and an average terrain height for each project were introduced into our AAT algorithm. For all runs a common set of control parameters of our AAT system, which govern the search radius for matching, the windows size for feature extraction and matching etc., was used.

The results are presented in form of tables. First we discuss the generation of multi-ray points and the point distribution. Besides the pixel size the average number of tie points per image and the number of multi-ray points is shown for each pyramid level and each data set in the Tables 2-6. The absolute numbers are rather large and guarantee a high redundancy in the robust bundle adjustment. The number of points increases between the start level and the intermediate level due to the increasing size of the images. Level 3 is chosen as intermediate level for all projects. From the intermediate level downwards the concept of backprojecting is applied together with the RANSAC algorithm, described in Section 2. The number of multi-ray points increases accordingly. While it is desirable to obtain many multi-ray points, it is also clear that the current implementation generated too many 2-ray points. One of the planned improvements is an intelligent selection of a reasonable amount of these points in order to improve the efficiency of the approach.

The point distribution during the tracking process was found to be stable. An example is shown in Figure 2 for the OEEPE–ISPRS test example OSU. Due to the large number of tie points only those with at least 4 rays were plotted. It can be seen that these points uniformly cover the whole block as desired. A quantitative analysis is provided in Table 7, in which the size of the area covered by 2, 3, 4, etc. images in comparison to the total block in percent is compared to the actual percentage of multi-ray points. Since in

Project	number of images	image scale	end / side overlap	scene description
Echallens	3 × 3	1:5000	60 % / 30 %	flat / open terrain
OSU	3 × 3	1:4000	60 % / 60 %	university campus / flat and buildings
Forssa	2 × 2	1:4000	60 % / 20 %	rural area / flat
München	3	1:2000	60 %	city centre
Manhattan	3	1:24000	60 %	inner city / high rise buildings

Table 1: Description of the test data

Pyramid level	pixel size [μm]	av. no. of pts per image	no. of multi-ray points in object space					
			total	2	3	4	5	6
6	1280	159	607	449	108	39	5	6
5	640	147	622	550	64	1	1	-
4	320	676	2841	2468	339	31	3	-
3	160	683	2272	1242	624	283	77	46
2	80	593	1919	967	578	248	79	47
1	40	560	1781	841	577	237	76	50
0	20	468	1591	839	534	163	43	12

Table 2: Point distribution for Echallens

Pyramid level	pixel size [μm]	av. no. of pts per image	no. of multi-ray points in object space								
			total	2	3	4	5	6	7	8	9
5	800	259	1067	897	148	19	1	2	-	-	-
4	400	451	1877	1623	206	41	3	4	-	-	-
3	200	511	1474	676	349	236	93	76	20	13	11
2	100	481	1335	529	366	219	100	79	21	11	10
1	50	443	1202	460	326	190	102	86	14	9	15
0	25	361	1055	485	262	160	76	46	7	15	4

Table 3: Point distribution for OSU

Pyramid level	pixel size [μm]	av. no. of pts per image	multi-ray points			
			total	2	3	4
5	960	143	284	279	4	1
4	480	480	941	908	25	8
3	240	429	766	618	111	37
2	120	335	587	457	94	36
1	60	276	485	378	78	29
0	30	216	376	282	74	20

Table 4: Point distribution for Forssa

Pyramid level	pixel size [μm]	av. no. of pts per image	multi-ray points		
			total	2	3
5	960	141	201	180	21
4	480	436	626	569	57
3	240	359	486	379	107
2	120	289	380	271	109
1	60	267	357	270	87
0	30	201	272	213	59

Table 5: Point distribution for München

Pyramid level	pixel size [μm]	av. no. of pts per image	multi-ray points		
			total	2	3
5	800	168	250	244	6
4	400	731	1072	1022	50
3	200	610	783	518	265
2	100	499	650	452	198
1	50	473	607	402	205
0	25	419	533	341	192

Table 6: Point distribution for Manhattan

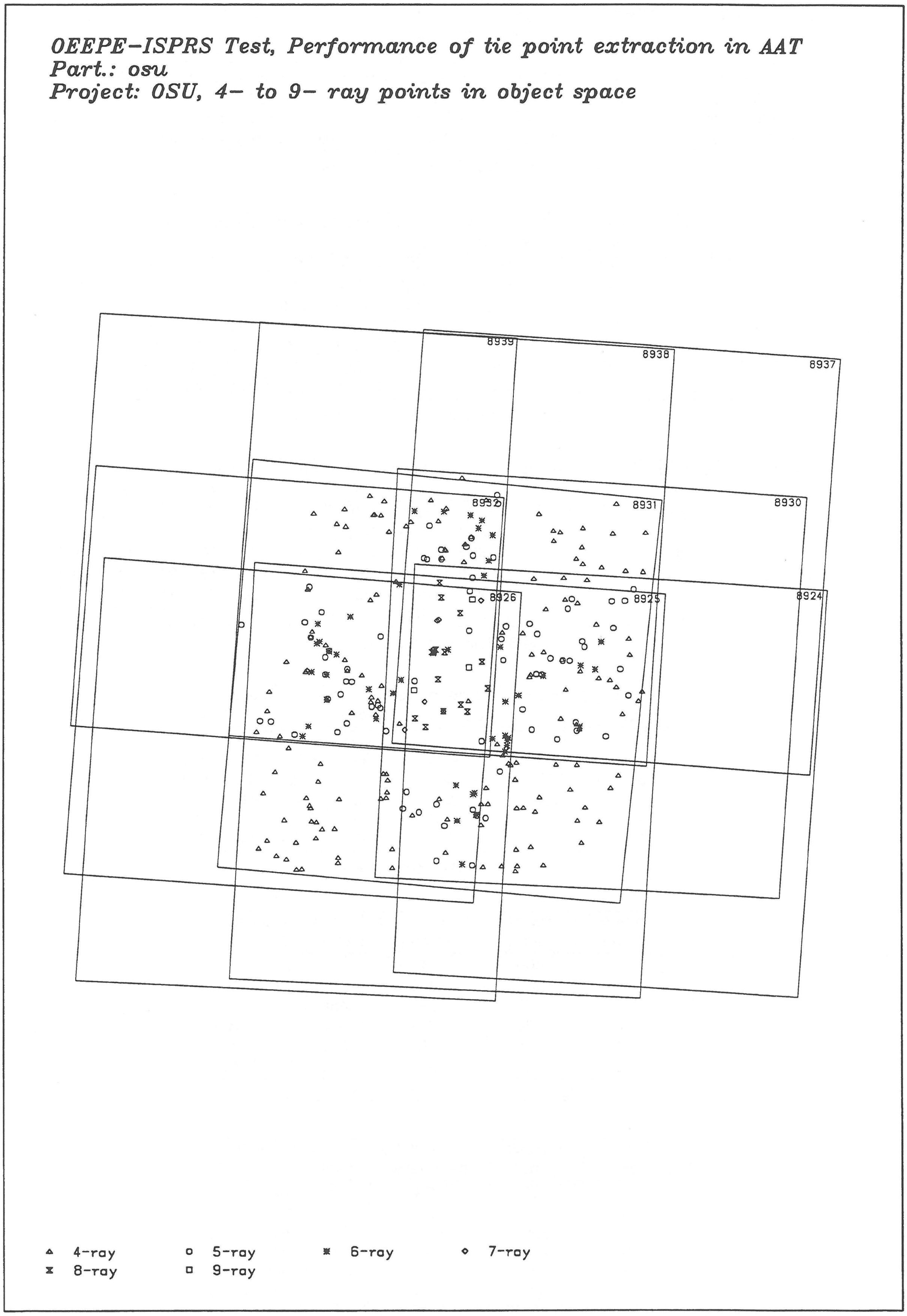

Figure 2: Point distribution in object space, example OSU

Project	multi-ray area in %, given the end and side overlap from Table 1					actual % of multi-ray points, see Tables 2-6				
	2	3	4	6	9	2	3	4	5+6	7+8+9
Echallens	67	12	17	4	-	53	34	10	3	-
OSU	50	12	25	12	1	46	25	15	12	2
Forssa	90	-	10	-	-	75	20	5	-	-
München	80	20	-	-	-	78	22	-	-	-
Manhattan	80	20	-	-	-	64	36	-	-	-

Table 7: Comparison between the multi-ray area given in % and the actual number of multi-ray points given in %

Project	pixel size [μm]	σ_0 [pixel]	σ_0 [μm]	σ_{FI} [μm]
Echallens	20	0.33	6.6	4.2
OSU	25	0.37	9.3	9.7
Forssa	30	0.32	9.7	-
München	30	0.33	9.8	7.5
Manhattan	25	0.32	8.0	-

Table 8: Test results

the standard block layout areas with 5-ray, 7-ray and 8-ray points do not appear, the corresponding percentages are summed up with 6-ray and 9-ray percentages respectively. It should be noted that these percentages must be interpreted with some care, since e.g. 3-ray points obviously occur not only in the 3-ray area but also in areas covered by more images. As can be seen, the percentage match rather well. For instance, for Echallens 3 % of 5- and 6-ray points were found, and the 6-ray area amounts to 4 %. Similar results were obtained for the other data sets, which is an indication that our focus on multi-ray points has been successfully integrated into the algorithm.

Second we focus on the accuracy results for the test images. Table 8 shows the standard deviation σ_0 of the tie points obtained at the original pyramid level in pixels and in μm. For the examples which were taken from the OEEPE-ISPRS test also a value σ_{FI} is given. σ_{FI} is the standard deviation for a set of manually measured reference tie points and can be regarded as an independent check of the computed orientation parameters. If σ_{FI} is in the order of or smaller than σ_0 the block orientation can be considered as correct. Further details can be found in (Heipke et al. 1998).

The obtained results for σ_0 lie between 0.32 and 0.37 pixels. Since only feature based matching was used , these results correspond with the expectations. The values in μm are somewhat inferior to those obtainable with natural points in analytical photogrammetry. It should be recalled, however, that the derived model points are not intended to be used in subsequent processing steps. The main result of AAT are the orientation parameters. They are determined with a much higher accuracy than in analytical photogrammetry due to the high redundancy (see also discussion in Ackermann, Krzystek 1997). The orientation parameters have been proven to be correct for the three projects of the OEEPE-ISPRS test as evidenced by the σ_{FI} value. For Forssa and Manhattan these independent tests are still pending.

4 CONCLUSIONS AND OUTLOOK

In this paper we have described a new concept for the generation of multi-ray points in automatic aerotriangulation. First experimental results serve as a proof-of-concept and demonstrate the feasibility of the concept. Further investigations will be directed towards increasing the accuracy of the tie point coordinates by introducing least-squares matching on the original image resolution and optimizing the performance of the approach. Also larger blocks will be treated. Since our approach is designed to work with frame and with 3-line imagery, tests on 3-line imagery will follow.

5 ACKNOWLEDGMENTS

Partial funding for this work was provided by the German Space Agency (DARA) under grant no. 50 QM 92053 and 50 QM 93077. This support is gratefully acknowledged.

6 REFERENCES

Ackermann, F., Krzystek, P. (1997): Complete automation of digital aerial triangulation. Photogrammetric Record (15) 89, pp. 645-656.

Fischler, M. A., Bolles, R. C., (1981): Random Sample Consensus : A Paradigm for Model Fitting with Applications to Image Analysis and Automated Cartography. Comm. ACM, 24(6), pp. 381–395, 1981.

Heipke, C., Eder, K. (1996): Performance of tie point extraction in automatic aerial triangulation. Description of the OEEPE-ISPRS test, Technical University Munich.

Heipke, C., Mayr, W., Wiedemann, C., Ebner, H. (1997): Automatic Aerotriangulation with Frame and Three-Line Imagery. In "Integrating Photogrammetric Techniques with Scene analysis and Machine Vision III", David M. McKeown, Jr., J. Chris McGlone, Olivier Jamet, Editors, Proceedings of SPIE Vol. 3072, pp. 286–294.

Heipke, C., Eder, K., Brand, R., Winkler, R. (1998): The OEEPE-ISPRS test " Performance of tie point extraction in automatic aerial triangulation"-Status and first results. International Archives of Photogrammetry and Remote Sensing, Vol. 32, Part B2.

Lue, Y., (1996): Towards a Higher Level of Automation for SoftPlotter. International Archives of Photogrammetry and Remote Sensing, Vol. 31, Part B3, pp. 478–483.

Miller, S.B., Paderes, F.C., Walker, A.S., (1996): Automation in Digital Photogrammetric Systems. International Archives of Photogrammetry and Remote Sensing, Vol. 31, Part B2, pp. 250–255.

Schenk, T., (1997): Towards automatic aerial triangulation. ISPRS Journal of Photogrammetry & Remote Sensing, Vol. 52, No. 3, pp. 110–121.

Schickler, W. (1992): Feature Matching for Outer Orientation of Single Images Using 3-D Wireframe Controlpoints. International Archives of Photogrammetry and Remote Sensing, Vol. 29, Part B3, pp. 591–598.

Tang, L., Heipke, C., (1996): Automatic Relative Orientation of Aerial Images. Photogrammetric Engineering & Remote Sensing, Vol. 62, No. 1, pp. 47–55.

Tang, L., Braun, J., Debitsch, R. (1997): Automatic aerotriangulation – concept, realization and results. ISPRS Journal of Photogrammetry & Remote Sensing, Vol. 52, No. 3, pp. 122–131.

Tsingas, V., (1992): Automatisierung der Punktübertragung in der Aerotriangulation durch mehrfache digitale Zuordnung. Deutsche Geodätische Kommission, C 392, 110 p.

Turau, V. (1996): Algorithmische Graphentheorie. Addison-Wesley, Bonn; Paris; Reading (Mass.) .

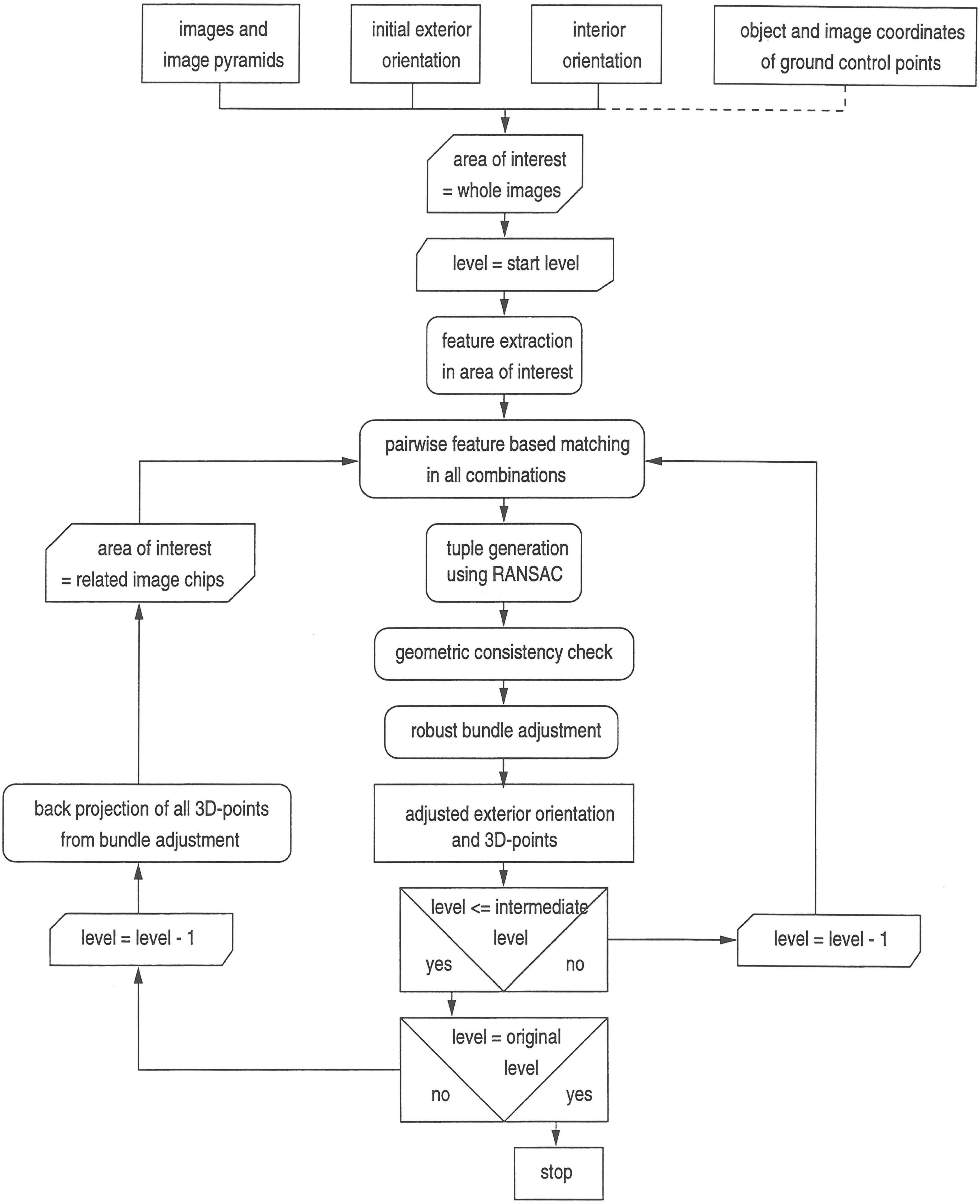
images and image pyramids
initial exterior orientation
interior orientation
object and image coordinates of ground control points
area of interest = whole images
level = start level
feature extraction in area of interest
pairwise feature based matching in all combinations
tuple generation using RANSAC
geometric consistency check
robust bundle adjustment
adjusted exterior orientation and 3D-points
level <= intermediate level
yes
no
level = level - 1
level = original level
no
yes
stop
level = level - 1
back projection of all 3D-points from bundle adjustment
area of interest = related image chips

OEEPE–ISPRS Test, Performance of tie point extraction in AAT
Part.: osu
Project: OSU, 4– to 9– ray points in object space

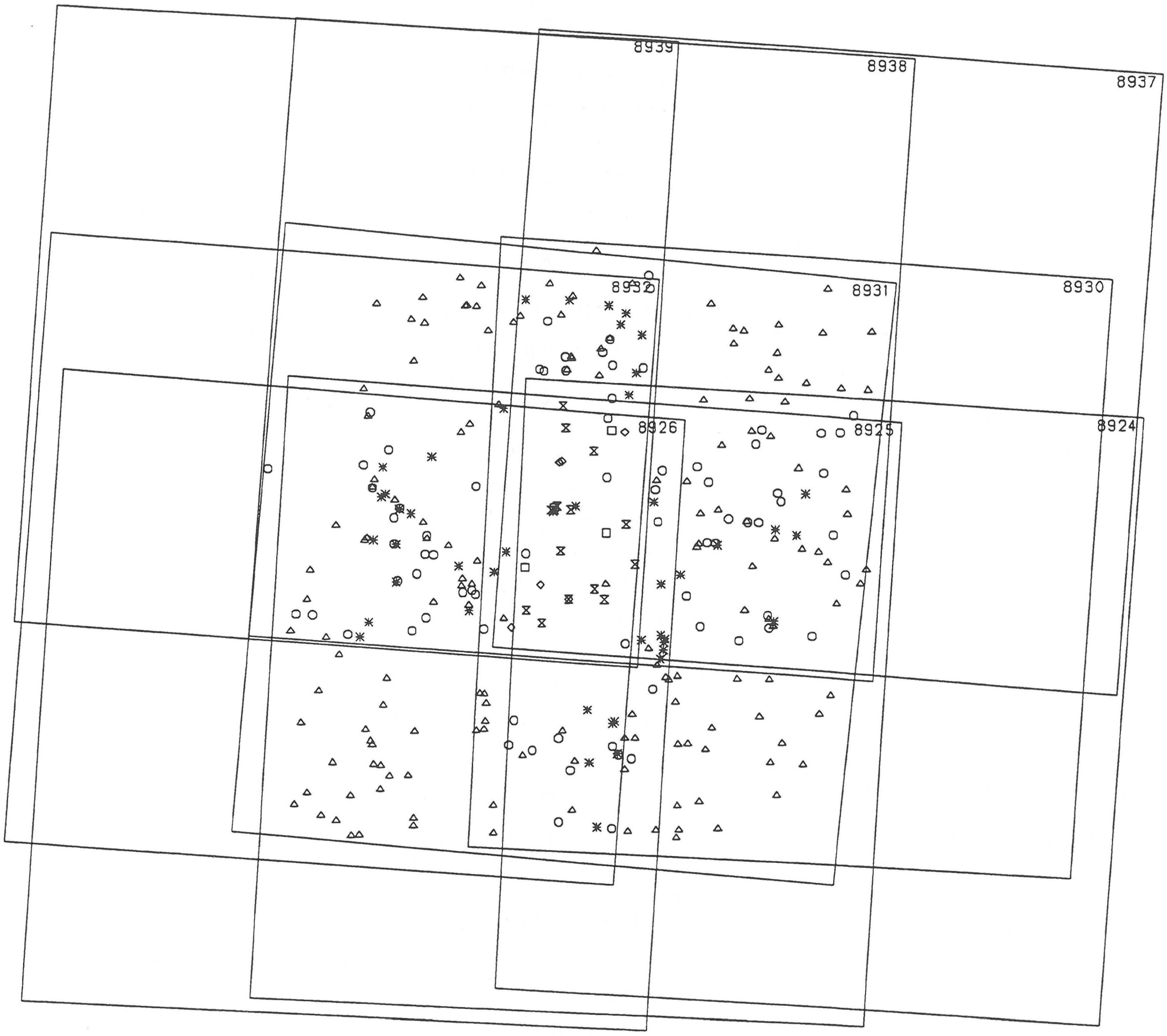

△ 4-ray ○ 5-ray ✳ 6-ray ◇ 7-ray
⧗ 8-ray □ 9-ray